Improved electrical and photoluminescence properties in Nd substitution of 0.94($Na_{0.5}Bi_{0.5}TiO_3$)-0.06BaTiO₃ lead free multi-functional ceramics

Kumara Raja Kandula, Sai Santosh Kumar Raavi*, Saket Asthana*

Advanced Functional Materials Laboratory, Department of Physics, Indian Institute of Technology Hyderabad Kandi (V), Sangareddy (Dist), Telangana 502285

*Corresponding author

Abstract

Nd^{3+}-substituted lead free 0.94 ($Na_{0.5}Bi_{0.5-x}Nd_XTiO_3$)-0.06BaTiO₃ (x=0, 0.01) ceramics were synthesized by using conventional solid state route. The XRD studies revealed the phase purity and existence of the monoclinic (Cc), cubic (Pm3m) along with the minor tetragonal phases confirmed with help of structural refinement. The electrical poling field induces the structural modification to rhombhohedral (R3c), cubic (Pm3m) along with the minor tetragonal phase (P4mm). The dielectric measurements revealed the relaxor behavior. The coercive field drops remarkable and there is slight improvement in the polarization with the substitution of Nd as compared to the pure 0.94($Na_{0.5}Bi_{0.5}TiO_3$)-0.06BaTiO₃. The luminescence occurred from the optically active element Nd^{3+} under the influence of the average crystal symmetry of 0.94($Na_{0.5}Bi_{0.5}TiO_3$)-0.06BaTiO₃. The luminescence quenching observed without any shift in position upon the poling supports the observation of higher symmetric structure. Copyright © 2018 VBRI Press.

Keywords: X-ray diffraction, dielectric, electromechanical coupling, polarization and photoluminescence.

Introduction

Near infrared luminescence phosphors materials have been known for its potential applications in the field of lightning industry, atmospheric transmission window, eye-safe laser radar and medical surgery process [1-3]. Among all other optically active luminescence centers, neodymium (Nd^{3+}) is the promising candidate for long range emission in infrared region [4]. The optical emission probability originates from the dipole transitions mainly decided by the host environment, which commonly decides by the lower phonon energy to avoid non-radiative transitions [5]. Now days the neodymium (Nd^{3+}) substituted phosphorous are being used in PLZT as laser-host active medium [6-7]. Even if Pb-based materials have an excellent ferro/piezoelectric property for suitable potential applications; those are highly toxic and hazardous restricted by Hazardous Substances Directive (*RoHS*)[8]. Among all lead free, sodium bismuth titanate (NBT) and its derivatives are the good candidates to replace lead based systems due to its lower phonon energy (540 cm⁻¹)[9,26].

In the present work, we have chosen 0.94($Na_{0.5}Bi_{0.5}TiO_3$)-0.06BaTiO₃ morphotropic system as a model host material due to its superior ferroelectric properties [10]. In order to improve the polarization conjunction with the lattice of this host, 1 mol (%) of Nd^{3+} substituted *(which we optimized through site specification method in NBT)* at Bi-site to maintain the charge balance [3]. The effect of electric poling is also explored to study the structural symmetry modification. The structural modulation due to electric poling influence the PL emission based on the structural symmetry.

Experimental

Polycrystalline Nd^{3+} Substituted 0.94($Na_{0.5}Bi_{0.5}TiO_3$)-0.06BaTiO₃ was synthesized with the help of conventional solid-state route by using high quality raw powders of Na_2CO_3, Bi_2O_3, Ba_2CO_3, TiO_2 and Nd_2O_3 (99.99% Sigma Aldrich Chemicals, USA) are weighed carefully according to stoichiometric ratios. Then after it milled and calcined at 800ºC for 3hrs. The calcined powders are further milled to break agglomerates and reduce the particle size for 10hrs with 300 rpm, sieved, and compacted into a circular pellet (φ=10 mm) and finally sintered at 1150°C for 3 hrs in air medium with a uniaxial rate of heating 5°C/min. The Single-phase formation was confirmed by using powder X-ray diffractometer (PANlyticalX'pertpro; CuK_α radiation λ = 1.5406Å) over the angle of 20°<2θ<80°. Relative density (RD) of the Nd^{3+} substituted 0.94 ($Na_{0.5}Bi_{0.5}TiO_3$)-0.06BaTiO₃ is measured using Archimedes method and estimated to be in the range of $94-95\%$ relative to the theoretical density of 5.94g/cm³. The polarization *(P)* vs electric field *(E)* measurements were performed using TF-Analyzer 2000 (aixACCT

systems, GmbH) on the silver coated samples. The sample was electrically poled at room temperature in silicon oil bath by applying a constant DC electric field of 3kV/mm for 30min. The room temperature PL spectrum was carried out in reflection mode by photo-exciting with 532nm from a cw-DPSS laser (LSR532NL-300, Lasever) and the subsequent PL is collected by a fiber coupled spectrometer (AvaSpec-ULS2048L-RS, Avantes) with a spectral resolution of 1.4nm.

Results and discussion

Fig. 1 shows the X-ray diffraction (XRD) patterns of polycrystalline ceramic powders, obtained from the unpoled and poled ceramics at electrical poling field of (3kV/cm) applied on the sintered ceramics. These ceramics are found pure crystalline phase in nature without any secondary phases within the sensitivity of the instrument. There is no evolution of additional peaks were observed in the presence of Nd^{3+} which reflects that the Nd^{3+} has diffused into the crystal lattice. The average structure of $0.94(Na_{0.5}Bi_{0.5}TiO_3)-0.06BaTiO_3$ near to its MPB, many different models have been reported in the existing literature. Several studies describe the structure of NBT-BT at MPB as a cubic or pseudocubic where a small tetragonal or rhombohedral distortion is possible [11-12]. The existence of different dual phase models have been suggested with Cc+Pm3m [13], Cc+P4bm [14], R3c+Pm-3m [15] and Cc+R3c [16]. The structural coexisting phase model of $0.94(Na_{0.5}Bi_{0.5}TiO_3)-0.06BaTiO_3$ was found to be monoclinic (Cc) and cubic (Pm3m) along with the slight distortion of tetragonal P4mm (2%), which is confirmed after scrutiny with different phase models. Here, by taking into consideration of all suggested models from the existing literature, a phase model Cc+P4mm+Pm3m was given the satisfactory fit along with the reasonable lattice parameters. The observed structural refined fit with the help of Cc+P4mm+Pm3m model is provided in **Fig.1(c)**. The poling field induces the structural change from model 1(Cc+P4mm+Pm3m) to model 2 (R3c+P4mm+Pm3m) [17] which can be clearly observable from the splitting of $(110)_{PC}$ reflection, as highlighted in the **Fig.1 (d and e)**. The electrically influenced structural modulation is resolved through the deconvolution of $(110)_{PC}$ peak.
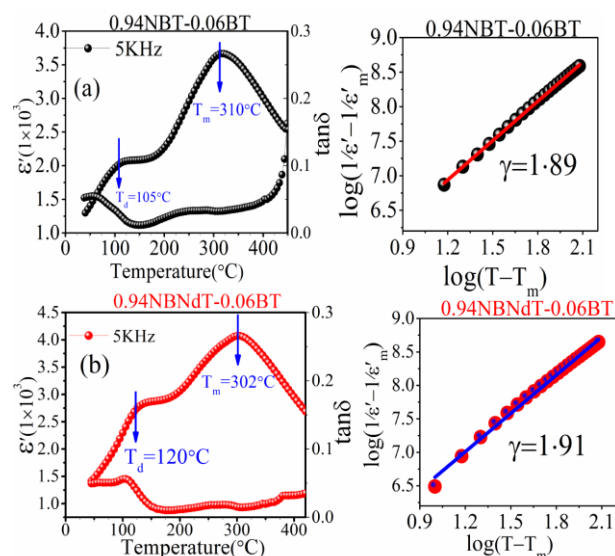
In order to understand the phase transition behavior of $0.94 (Na_{0.5}Bi_{0.5-x}Nd_xTiO_3)-0.06BaTiO_3$ (x=0, 0.01) over the variation of temperature, the temperature dependent dielectric constant and loss tangent(tanδ) at 5KHz are shown in **Fig. 2a** and **2b,** respectively). There are two prominent dielectric anomalies, corresponding to temperatures T_d (depolarization temperature) and T_m (maximum temperature), those are the responsible for the phase transitions from ferroelectric to antiferroelectric and antiferroelectric to paraelectric over the temperature range. The T_d and T_m were found to be 105°C, 120°C and 310°C, 302°C for the x = 0 and x = 0.01), respectively. The substitution of Nd facilitates

to improve the long range ferroelectric region, which is observed from the enhanced T_d compared with the x=0. Above T_d, long range ferroelectric order can be disrupted. The temperature beyond T_m the nature of dielectric curve behavior
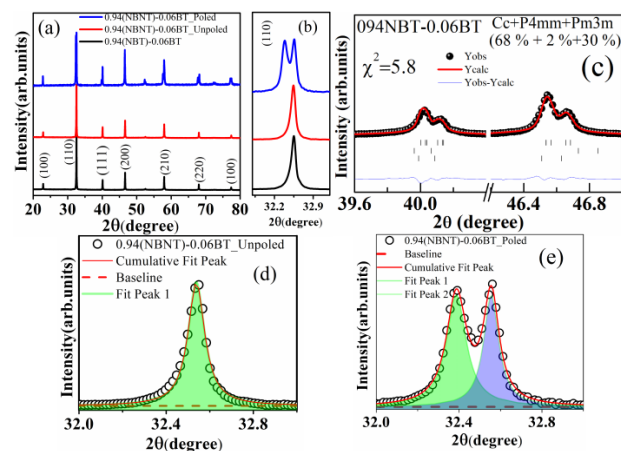
Fig.1. (a-b) XRD pattern of Polycrystalline ceramic powders of $0.94(Na_{0.5}Bi_{0.5-x}Nd_xTiO_3)-0.06BaTiO_3$ (x=0, 0.01), poled (x=0.01) and zoomed pattern of main intense peak $(110)_{PC}$. (c) Refinement pattern of x=0 with the phase model Cc+P4mm+Pm3m. (d-e) the peak deconvolution of particular $(110)_{PC}$ reflection to observe the structural modulation over the electrical poling on x=0.01.

responsible for the association of relaxation of polar nano- regions (PNRs), which are emerging from the lower symmetry Cc [18]. The relaxation behavior estimated with the help of the diffusiveness coefficient γ followed by the equation$(1/\varepsilon - 1/\varepsilon') + \ln C = \gamma \ln(T - Tm)$. Here, it is worth to highlight that relaxor behavior is almost invariant with Nd substitution which is supported by insignificant increase in the γ value [19].

Fig. 2. (a-b) Temperature dependent of dielectric constant (ε') and loss tan (δ) in the temperature range from room temperature to 420°C for $0.94(Na_{0.5}Bi_{0.5-x}Nd_xTiO_3)-0.06BaTiO_3$ (x=0, 0.01) and the corresponding diffusivity γ represents respectively.

In order to understand the dipole response of these dense ceramics under the electrical poling field, the electromechanical coupling factor (K_p) has been estimated with the help of following equation [20]. Here, K_P value measured by using f_r (*resonance frequency*) and f_a (*anti-resonance frequency*) are extracted from the room temperature capacitance vs frequency measurement carried on poled ceramics at poling field of 3kV/cm. The electromechanical coupling factor Kp values show maximum for x=0.01 compared to the x = 0, reflects the domain switching behavior in presence of Nd.
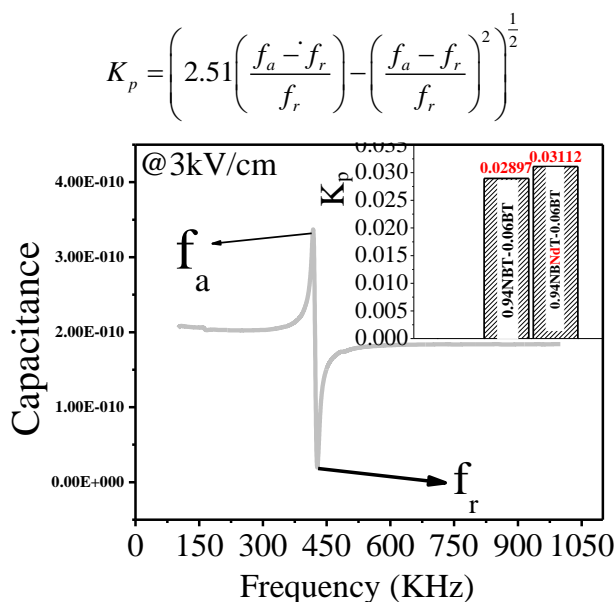
$$K_p = \left[2.51\left(\frac{f_a - f_r}{f_r} \right) - \left(\frac{f_a - f_r}{f_r} \right)^2 \right]^{\frac{1}{2}}$$

Fig. 3. Estimation of electromechanical coupling coefficient (K_P) for $0.94(Na_{0.5}Bi_{0.5-x}Nd_xTiO_3)$-$0.06BaTiO_3$ (x=0, 0.01) at 3kV/mm poling field respectively.

Room temperature polarization (P) versus electric field (E) hysteresis loop measured for both 0.94 $(Na_{0.5}Bi_{0.5-x}Nd_xTiO_3)$-$0.06BaTiO_3$ (x=0, 0.01) specimen depicts well saturated and squared loops with slight increment in remnant polarization(P_r), drop in coercive field (E_c) 39kV/cm to 29kV/cm:

$$R_{sq} = \left(\frac{P_r}{P_s} \right) + \left(\frac{P_{1.1E_C}}{P_r} \right)$$

$(\Delta E_c = 10kV/cm)$ for x = 0.01Since the lower coercive field Ec value is obtained in the presence of Nd^{3+}, facilitates in the movement of domain, which causes improved ferroelectric property. The squareness of the hysteresis loops can be estimated quantitatively with the help of following equation [3].

Here the squareness of hysteresis loop (R_{sq}) is estimated with the help of remnant polarization(P_r), saturated polarization(P_s) at finite field strength and $P_{1:1\ EC}$ is the polarization at the field equal to$1.1Ec$. For an ideal square loop, the typical, R_{sq} value close to 2 [21]. We have noticed the estimated values for these specimens are 1.82 and 1.79 for x=0 and 0.01 respectively, those values are within the vicinity of the

ideal square loop. In addition to that the sharp switching current observed from I-V curve for both specimens reflects the strong ferroelectric behavior. The maximum sharp I-V curve well coincides with a coercive field of respective compositions [22]. The substitution of Nd will facilitate the domain wall switching more compared to x = 0.
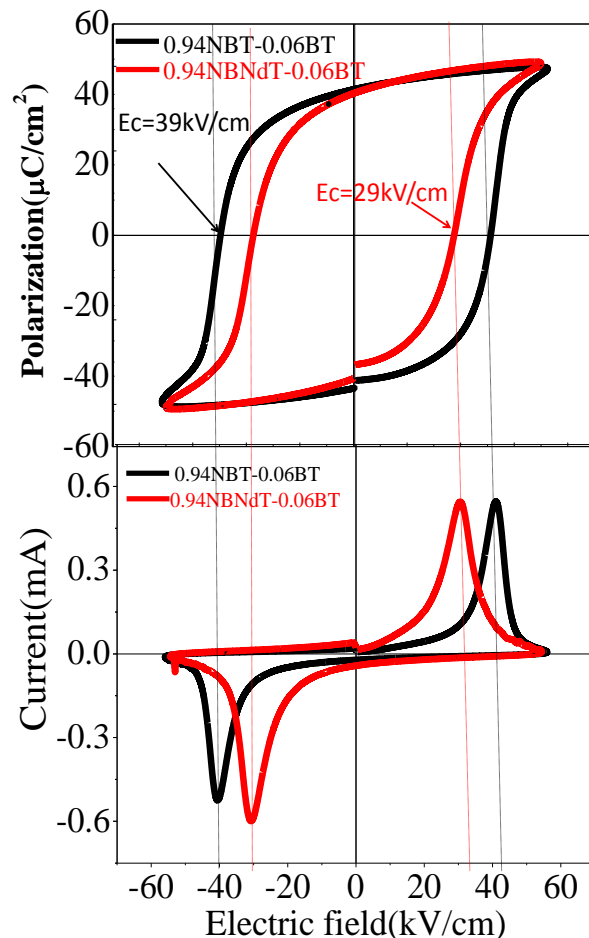

Fig. 4. Room temperature polarization (P) versus electric field (E) hysteresis and I-V characteristic curve for $0.94(Na_{0.5}Bi_{0.5-x}Nd_xTiO_3)$-$0.06BaTiO_3$ (x=0, 0.01) respectively.

The room temperature photoluminescence (PL) spectra of $0.94(Na_{0.5}Bi_{0.5-x}Nd_xTiO_3)$-$0.06BaTiO_3$ (x = 0, 0.01) and x = 0.01 poled at 3kV/mm carried upon the excitation of 532nm. The PL signal observed from the x = 0.01, present in the **Fig. 5** and there is no signal observed from the x=0. The obtained luminescence intensity mainly originates from the radiative transition attributable to electrical dipole transitions among 4f-4f of Nd^{3+}. The yield originates from the probability of dipole transitions of Nd^{3+}. The probability density will facilitate under the ferroelectric crystal field environment because of 4f–4f electric dipole transitions are forbidden. The emission lines in the different wavelength range are categorized as $4F_{3/2} \rightarrow {}^4I_{9/2}$ (884 nm and 915 nm) and around due to the $^4F_{3/2} \rightarrow {}^4I_{11/2}$(1064nm) [23]. The better yield is observed under the influence of NBT-BT crystal field environment

compared to NBT because of the lower phonon energy of NBT-BT ($420 cm^{-1}$) and NBT ($540 cm^{-1}$)[24]. The luminescence intensity quenching upon the poling due to the structural modification from lower symmetry (Cc+P4mm+Pm3m) to higher symmetry (R3c+P4mm+Pm3m) supports the Judd-ofelt theory [25].
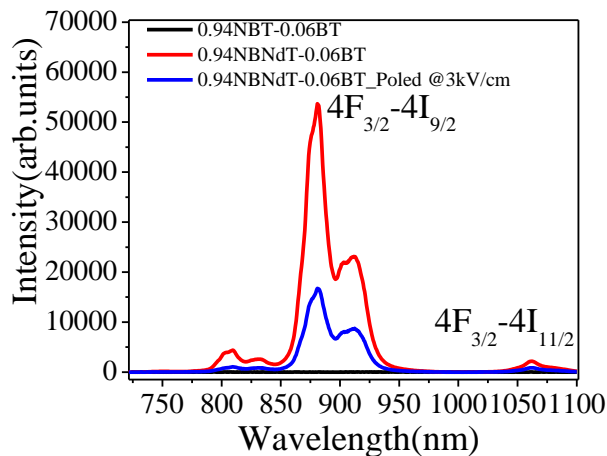
Fig. 5. Room temperature photoluminescence spectra of 0.94 $(Na_{0.5}Bi_{0.5-x}Nd_xTiO_3)$-$0.06BaTiO_3$ (x=0, 0.01) and poled x = 0.01 at 3kV/mm respectively.

Conclusion

The lead free $0.94(Na_{0.5}Bi_{0.5-x}Nd_xTiO_3)$-$0.06BaTiO_3$ (x = 0, 0.01) were synthesized successfully with the help of solid state reaction route. The structural phase purity and existence of structural phase model (Cc+P4mm+Pm3m) confirmed by using rietveld refinement. The poling field induces the structural modulation to (R3c+P4mm+Pm3m).The temperature dependence dielectric measurements revealed the relaxor behavior. The substitution of Nd will facilitates the domain wall switching reflects from the electromechanical coupling coefficient (K_p) as well the change in the coercivity ($\Delta E_c = 10kV/cm$) in between x = 0 and x = 0.01. The luminescence suffers due to the structural symmetry modification upon poling from (Cc+P4mm+Pm3m) to (R3c+P4mm+Pm3m).

References

1. Jackson S.D. *Nature photonics*. **2012**, 6(7), 423-31.
2. Tian. Y, Zhang. J, Jing. X, Xu. S. *J. Mater. Sci. Mater. Electron*. **2013**,24(3), 866-70.
3. Kandula K.R, Raavi.S. S, Asthana.S. *J. Alloy.Comp*.**2018,** 25, 732:233-9.
4. Chen. F. F, Wei. H. B, Bian. Z. Q, Liu. Z. W, Ma. E. *Organometallics*. **2014**, 33(13), 3275-82.
5. Zhang. Z, Shen. D.Y, Boyland A.J, Sahu J.K. *Opt.lett*. **2008**, 33(18), 2059-61.
6. Singh. G, Tiwari. V.S, Sharma. T.K, Gupta. P.K. *J. Electroceramics*. **2010** 25(1), 89-92.
7. Singh. G, Selvamani. R, Tiwari. V.S, Karnal. A.K. *J. Lumin*. **2017**, 192, 1084-8.
8. Directive E.U. *Official Journal L*. **2002**, 37,13.
9. Du. P, Yu J.S. *Ceram. Intern*. **2015,** 41(5), 6710-4.
10. Seo I.T, Steiner.S, Frömling.T. *J. Eur. Cerm. Soc*. **2017**, 37(4), 1429-36.
11. Daniels J.E, Jo. W, Rödel. J, Jones J.L. *Appl. Phys. Lett*. **2009**, 95(3), 032904.
12. Zhang S.T, Kounga A.B, Aulbach. E, Ehrenberg. H, Rödel. *Appl. Phys.Lett*.**2007**, 91(11), 112906.
13. Usher T.M, ForresterJ.S, Jones J.L. *Appl. Phys. Lett*. **2012**, 101(15), 152906.
14. Ge. W, Luo. C, Zhang. Q, Ren.Y, Li. J. *Appl. Phys. Lett*. **2014,** 105(16), 162913.
15. Garg. R, Rao B.N, Senyshyn. A, Krishna PS, Ranjan R. *Phys. Rev. B*. **2013**, 88(1), 014103.
16. Maurya. D, Murayama. M, Pramanick.W.T.J.*Appl. Phys*. **2013,** 113(11), 114101.
17. Rao B.N, Avdeev. M, Kennedy. B, Ranjan. R. *Phys. Rev. B*. **2015,** 92(21), 214107.
18. Maurya. D, Pramanick. A, Feygenson. M. *J. Mater. Chem. C*. **2014**, 2(39), 8423-31.
19. Uchino.K, Nomura.S. *Ferroelectrics*.**1982**, 44(1), 55-61.
20. Wathore N.N, Lonkar C.M, Kharat D.K. *Bull. Mater. Sci*. **2011**, 34(1), 129-32.
21. Aksel. E, Jakes. P, Erdem. E, Smyth D. M, A. *J. Amer. Ceram. Soc*. **2011,** 94(5), 1363-7.
22. Kandula K.R, Raavi S.S, Asthana.S. *Ferroelectrics*. **2017**, 518(1), 23-30.
23. Zannen. M, Lahmar. A, Dietze. M, Khemakhem. H, Kabadou. A. *Mater.Chem.Phys*.**2012**, 134(2), 829-33.
24. Datta. K, Richter. A, Göbbels. *Phys. Rev. B*. **2014**, 90(6), 064112.
25. Singh. G, Selvamani. R, Tiwari V.S, Karnal A.K. *J. Lumi*. **2017,**192,1084-8.
26. Kandula K.R, Raavi.S.S, Asthana. S. *Phys. Stat. solidi (a)*. **2018**.